Annealing of ^{60}Co gamma radiation-induced damage in *n*-GaN Schottky barrier diodes

G. A. Umana-Membreno, J. M. Dell, G. Parish, B. D. Nener, and L. Faraone
School of Electrical, Electronic and Computer Engineering, The University of Western Australia, Crawley WA 6009, Australia

S. Keller and U. K. Mishra
Department of Electrical and Computer Engineering, University of California, Santa Barbara, California 93106

(Received 20 November 2006; accepted 13 December 2006; published online 8 March 2007)

The effect of isochronal thermal annealing on Ni/n-GaN Schottky barrier diodes exposed to a total accumulated gamma-ray dose of 21 Mrad(Si) has been investigated using capacitance-voltage (C-V) and current-voltage (I-V) measurements, while capacitance deep-level transient spectroscopy (DLTS) has been employed to monitor the evolution and annihilation of radiation-induced defects during thermal annealing. Annealing temperatures up 160 °C were found to improve device I-V characteristics; however, thermal annealing above 250 °C resulted in: (a) Degradation of both forward and reverse I-V characteristics, (b) reduction in free carrier concentration, and (c) a decrease in the concentration of radiation-induced defects, as evidenced by DLTS measurements. Following annealing above 350 °C, the radiation-induced defects were no longer detectable using DLTS. Analysis of the thermally induced reduction in radiation-induced defect concentration indicated that the dominant defect-annihilation process has a mean activation energy of 1.8 eV. The physical origin of radiation-induced defects, and of defects involved in their annihilation process, is discussed in the perspective of published theoretical calculations of native defect diffusion mechanisms in GaN.
 [DOI: 10.1063/1.2435972]

I. INTRODUCTION

Gallium nitride and related wide-band gap semiconductor alloys are important for the fabrication of short-wavelength light emitters and detectors. The low intrinsic carrier generation rates and high breakdown fields, which are a consequence of the wide energy gap of GaN-based alloys, make this material system attractive for the fabrication of microelectronic devices capable of reliable operation at high power/voltage levels, at high temperatures, and in high-energy radiation environments.[1,2] For applications involving significant radiation exposure, such as in aerospace, medicine, military, and nuclear applications, the study of high-energy irradiation effects on device performance is essential to assess long-term device reliability and develop radiation-tolerant circuits and systems.

Exposure of GaN semiconducting films to energetic particle irradiation invariably results in the introduction of vacancy and interstitial point-defects by displacement of N and Ga species from their respective sublattices. However, the isolated character of these defects may be modified by thermally activated defect migration and interactions with native defects even at temperatures near 300 K. The evolution from isolated point defects, as initially introduced by irradiation at cryogenic temperatures, to more complex defect structures has been clearly evidenced by electron paramagnetic resonance studies of electron-irradiated GaN films.[2–5] These studies have also provided unambiguous identification of Ga interstitials (Ga_I), established that such defects are mobile at near ambient temperatures and that they manifest electronically stimulated migration at cryogenic temperatures.[2,5,6] In contrast, positron annihilation spectroscopy studies have shown that isolated Ga vacancies (V_{Ga}) in n-GaN and N vacancy (V_{N}) related complexes in p-type GaN become mobile in the temperature ranges of 200–350 and 500–800 °C, respectively.[7,8]

Similar to other semiconductor materials, the introduction of radiation-induced defects in GaN films invariably results in the creation of levels in the forbidden energy gap that may act as scattering centers and as either donors, acceptors, traps, or recombination centers, thereby affecting the electronic and optical material properties and, consequently, semiconductor device performance.[9–16] At sufficiently high concentrations, radiation-induced defects have been shown to result in degradation of carrier mobility and changes in free carrier concentration, which vary with the material doping level, an indication that irradiation-induced point defects may interact with impurities as well as native defects.[17–19] From changes in the magnetotransport properties of electron-irradiated n-GaN films, Look and co-workers[17] identified V_{N} as a radiation-induced shallow donor with a thermal activation energy of 0.07 eV, and noted that thermal annealing at 200–400 °C induced a complete recovery of the radiation-induced mobility degradation. These observations were attributed to recombination of radiation-induced V_{N} and N interstitial (N_I) pairs.[17] Emtsev *et al.*[18] found a more complex post-irradiation thermal annealing behavior in both doped and undoped n-GaN layers, which was interpreted as an indication that the process of defect annihilation occurs via interactions with native defects and/or impurities. This view appears to be supported by the complex carrier emission characteristics of radiation-induced defects in n-GaN, as detected by deep-level transient spectroscopy (DLTS) techniques.[15,20–22]

The relatively high irradiation doses employed in most published studies of GaN, which have been necessary in order to induce sufficiently high defect concentrations, indicate low defect production rates and high energy thresholds for displacement damage. Such studies confirm the potential of GaN-related materials and devices to be used in circuit and system applications requiring radiation-hardness. However, even though low susceptibility of bulk material to radiation damage is fundamental to achieve radiation-hard devices, the radiation tolerance of electronic devices and circuits is usually limited by radiation-induced effects associated with electrical contacts, surfaces and interfaces, and the presence of extended defects such as dislocations.[23,24] For the case of GaN-based alloys, there are still relatively few published reports on the effects of post-irradiation thermal annealing on metal-GaN Schottky contacts, which constitute a critical element of metal-semiconductor field-effect transistors and heterostructure-based high electron mobility field-effect transistors, even though most DLTS studies of radiation-induced defects in n-GaN have been undertaken using Schottky-barrier diodes. One of the earliest indications of radiation-induced degradation of Schottky contacts to GaN can be found in the reports of Fang *et al.* and Polenta *et al.*, who noted that device degradation induced by exposure to 1 MeV electrons could be annealed by prolonged storage at room temperature, which resulted in a recovery of device characteristics and reduction in the concentration of radiation-induced defects.[21,25] Irradiation with different energetic particles has been found to produce similar defects in n-GaN, and their annealing behavior has been found to coincide with a recovery in forward bias current-voltage (I-V) device characteristics.[26] Previously, we have reported on the effects ^{60}Co gamma-irradiation induced defects on the characteristics of Ni/GaN Schottky diodes.[15] Device irradiation was found to cause an apparent increase in the value of the Schottky barrier height extracted from capacitance-voltage (C-V) measurements, and to result in significant degradation in reverse bias dc I-V characteristics. However, the barrier height extracted from forward bias I-V characteristics remained essentially constant for total radiation doses up to 21 Mrad(Si). Post-irradiation storage at room temperature for six days and subsequent thermal annealing for 15 min. at 50 °C was found to fully recover the reverse bias I-V characteristics to pre-irradiation levels without having any significant effect on (i) the C-V characteristics, (ii) forward bias dc I-V characteristics, or (iii) the parameters of the radiation-induced defect levels detected by DLTS.[15]

In this paper, we present results of a study on the effect of isochronal thermal annealing on ^{60}Co gamma-irradiated Ni/n-GaN Schottky barrier diodes. The effect of thermal annealing on device characteristics has been investigated using C-V and I-V measurements, while transient capacitance DLTS has been employed to monitor the evolution and/or annihilation of radiation-induced defects.

II. SAMPLE PREPARATION AND EXPERIMENTAL DETAILS

Schottky-barrier diodes were fabricated on a 2 μm thick nominally undoped GaN epitaxial layer grown at the University of California at Santa Barbara by metal-organic chemical vapor deposition on a sapphire substrate.[27] The devices were defined by alloyed Al/Cr/Au ohmic contacts and subsequently-formed coplanar Ni/Au Schottky contacts of 600 μm diameter, with a separation of 30 μm over which the GaN surface was not passivated. The devices were exposed to a total dose of 21 Mrad(Si) ^{60}Co gamma-rays at an average dose rate of 2 krad(Si)/min in a nitrogen ambient at room temperature. As previously reported,[15] measurements performed following the maximum total dose of 21 Mrad(Si) and after sample storage at room temperature for six days followed by thermal annealing for 15 min at 50 °C indicated a complete recovery of reverse dc I-V characteristics to pre-irradiation levels, whereas the post-irradiation C-V characteristics and DLTS parameters of the radiation-induced defect centers were unaffected.

In the present study, a series of consecutive post-irradiation thermal anneals were performed for 30 min in a N_2 ambient at temperatures ranging from 80 to 350 °C. After each anneal, the room-temperature C-V and I-V device characteristics were measured under dark conditions using a HP 4280A 1 MHz C-V meter and a HP 4145B Semiconductor Parameter Analyzer, respectively. Since the signals associated with carrier emission from the radiation-induced defects could only be detected from 60 to 150 K, DLTS measurements were limited to this temperature range. The DLTS measurements were performed isothermally by sampling the capacitance transients resulting from a 10 s voltage pulse (V_P) to 0 V from a quiescent reverse bias (V_R) of 5 V; such a long trap-priming pulse was necessary in order to ensure observation of the combined emission signal resulting from the various radiation-induced charge trapping centers.

III. EXPERIMENTAL RESULTS AND DISCUSSION

A. *C-V* and *I-V* characteristics

Analysis of experimental diode C-V characteristics was performed using the usual expression for the bias-dependent depletion capacitance per unit area C of an ideal Schottky barrier diode

$$C^{-2} = \frac{2}{q\varepsilon_s N}(V_{d0} - V), \tag{1}$$

$$V_{d0} = \phi_B^{cv} - (k_B T/q)\ln(N_c/N) - k_B T/q, \tag{2}$$

where V and T are the applied bias and device temperature, respectively, q is the electronic charge constant, k_B is Boltzmann's constant, ε_s is the permittivity of GaN ($9.5\varepsilon_0$), V_{d0} is the zero-bias diffusion potential, ϕ_B^{cv} is the flat-band Schottky barrier height, N_c is the effective density of states in the conduction band (for GaN, $N_c = 2.6 \times 10^{18}$ cm^{-3} at 300 K) and N is the free electron concentration. For a uniform carrier concentration, C^{-2} is a linear function of V with a gradient of $-2/(q\varepsilon_s N)$ and an intercept with the V axis of

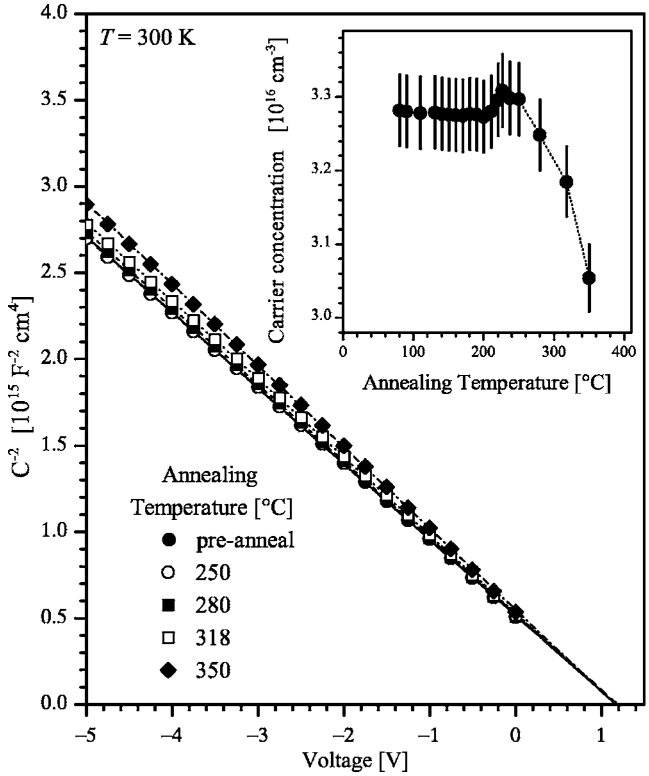

FIG. 1. Effect of isochronal thermal annealing on C^{-2}-V diode characteristics (for clarity, one in every five experimental data points is shown). Note the constant voltage-axis intercept and the increase in gradient for annealing temperatures ≥250 °C. Inset: Free electron concentration as a function of annealing temperature.

$V_{d0}-k_BT/q$, where ϕ_B^{cv} can be extracted with the aid of Eq. (2).

As indicated by the C-V data plotted in Fig. 1, the dominant effect of thermal annealing on the post-irradiation characteristics is an increase in the gradient of C^{-2}-V for annealing temperatures above 250 °C, which translates to an accumulated decrease of 7±3% in carrier concentration after the final 350 °C anneal (see inset in Fig. 1). While a marginal decrease in the C-V Schottky barrier height, ϕ_B^{cv}, is also observed after annealing in above 250 °C (see Fig. 2), the error bounds of the extracted parameter ϕ_B^{cv} indicate that ϕ_B^{cv} remains unchanged from its post-irradiation value of 1.30±0.03 eV for all annealing temperatures. This is also evident from the nearly constant voltage-axis intercept of C^{-2} shown in Fig. 1.

The effective zero-bias Schottky barrier height, ϕ_{B0}^{iv}, and diode ideality factor, n, were extracted from forward bias I-V measurements using the conventional thermionic-emission model[28]

$$I = AJ_s \exp\left(\frac{qV}{nk_BT}\right)\left[1-\exp\left(-\frac{qV}{k_BT}\right)\right], \tag{3}$$

$$J_s = A^{**}T^2 \exp\left(-\frac{\phi_{B0}^{iv}}{k_BT}\right), \tag{4}$$

where A is the device active area, J_s is the saturation current density, and A^{**} is the effective Richardson constant. The effect of series resistance, R_s, can be incorporated in (3) by replacing V with $V-IR_s$. Curve-fitting was performed numerically using an effective Richardson constant of $A^{**}=26.4\ \mathrm{cm}^{-2}\ \mathrm{K}^{-2}(m_e=0.22)$ to extract ϕ_{B0}^{iv}.

From the post-irradiation forward I-V characteristics, consecutive isochronal anneals up to about 250 °C were found to induce a marginal increase in effective Schottky barrier height ϕ_{B0}^{iv} from 1.13±0.01 eV [after 21 Mrad(Si) accumulated gamma-ray dose], to 1.16±0.02 eV after annealing up to 250 °C. Over the same annealing temperature range, n and R_s were noted to remain approximately constant at 1.14±0.01 and 49±2 Ω, respectively. As evident from the I-V curves in Fig. 3, further isochronal annealing at temperatures ≥250 °C resulted in significant degradation in the forward I-V characteristics. This degradation, evident as an increase in current levels at low values of forward bias, is characterized by ϕ_{B0}^{iv} decreasing from 1.16±0.02 eV to 0.97±0.02 eV after consecutive anneals in the range from 250 °C to 350 °C, with a corresponding increase in n from 1.14±0.01 to 1.50±0.02 (see inset in Fig. 3) and in R_s from 49±2 Ω to 52±2 Ω. In contrast, the reverse I-V characteristics were found to be virtually unaffected by thermal anneals up to 160 °C, as evident from Fig. 4. Subsequent higher temperature isochronal annealing resulted in significant degradation in reverse leakage current, which was more severe at higher levels of reverse bias.

The degradation observed in I-V characteristics for annealing temperatures above 250 °C coincides with the temperature range over which C-V measurements indicate a decrease in carrier concentration but no significant change in barrier height. However, the decrease in carrier concentration of approximately 7% is unlikely to have any significant influence on the forward I-V characteristics, since R_s in the present samples is dominated by contact resistance rather than by the sheet resistance of the GaN epitaxial layer. On the other hand, the differences between the extracted ϕ_{B0}^{iv} and ϕ_B^{cv} combined with the large values of ideality factor for annealing above 250 °C cannot be attributed to image-force barrier lowering, since the maximum corrections to ϕ_{B0}^{iv} and n are estimated to be $\Delta\phi_B<0.06$ eV and $\Delta n<0.02$. While such discrepancies are not surprising in view of the nonidealities reported in most studies of metal/n-GaN Schottky barrier diodes,[29–32] in the present study the difference in I-V and C-V extracted barrier heights is primarily due to radiation-induced changes. For example, and as shown in Fig. 2, ϕ_B^{cv} was found to increase from 1.14±0.02 to 1.30±0.01 eV after a cumulative gamma-ray dose of 21 Mrad(Si), whereas ϕ_{B0}^{iv} remained essentially constant with irradiation exposure.[15]

In previous studies, the nonideal electrical characteristics of as-fabricated GaN Schottky diodes and, in particular, the scatter in the reported barrier height of Ni/GaN contacts, have been proposed to be attributable to surface-states and interfacial defects, dislocation-related current paths, interfacial layers induced by metal/GaN reactions or surface preparation, and material nonuniformity and quality.[29,33–41] While a combination of the above is also likely to play a role in the present samples, defects such as dislocations and interfacial states are of particular relevance to this study because irra-

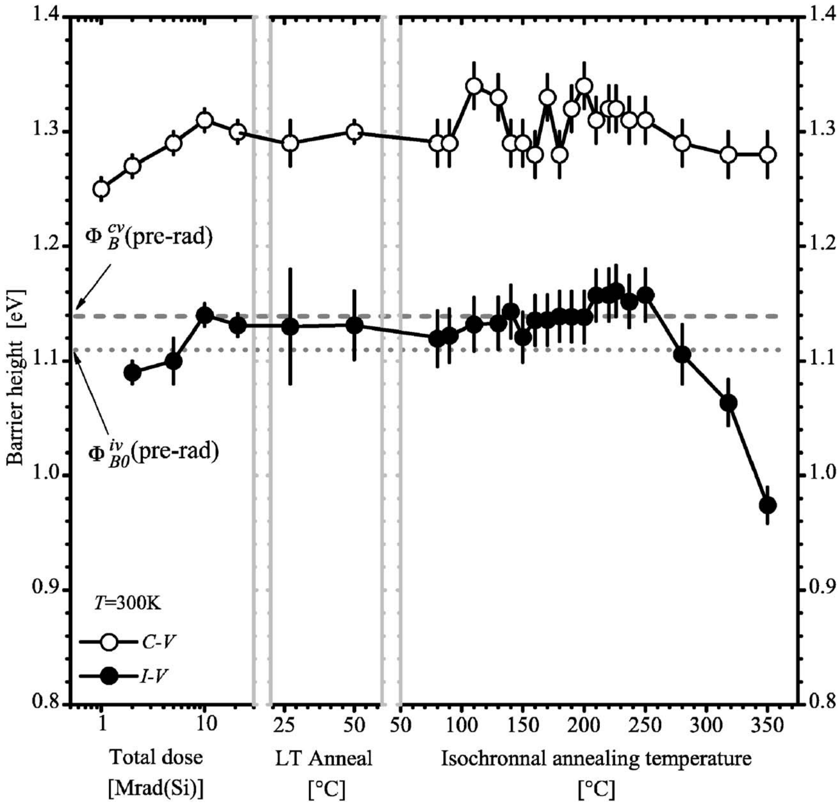

FIG. 2. Summary of extracted Schottky-barrier height from *I-V* and *C-V* measurements after ^{60}Co gamma-irradiation exposure and after post-irradiation thermal treatment. The pre-irradiation barrier heights are indicated by the dotted and dashed lines. LT anneal denotes storage at 27 °C for six days, and thermal annealing in N_2 ambient for 15 min at 50 °C. The isochronal annealing time was 30 min with each anneal performed consecutively at an increasing temperature in the N_2 ambient.

diation and/or post-irradiation annealing are likely to have a significant influence on effects associated with such defects.

Electrically active dislocations are known to affect the characteristics of Schottky barrier diodes mainly by acting as efficient current leakage paths across the depletion layer and metal/GaN interface.[36–38,42,43] There is evidence from previous studies suggesting that the electrical activity at dislocations is correlated with defects and impurities trapped in their stress field,[44,45] and that the Schottky barrier height in localized regions near or at the surface termination of dislocations is lower than in dislocation-free regions.[36] It has also been reported that while the physical surface termination of active dislocations tends to be dimensionally small, with diameters

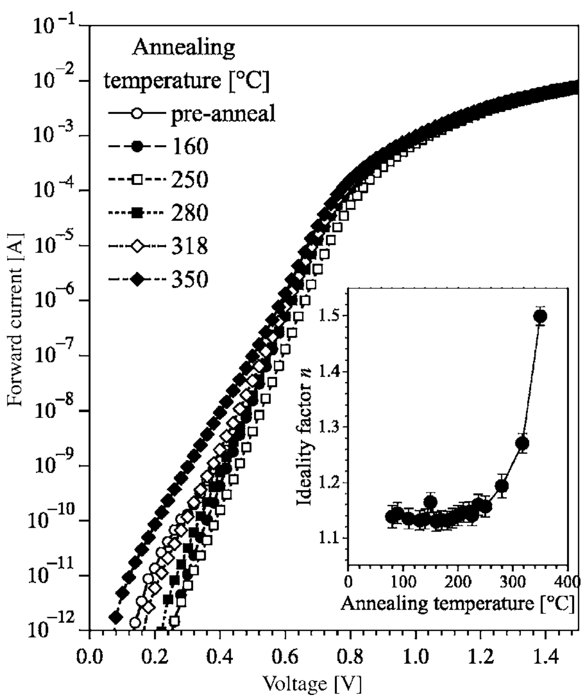

FIG. 3. Effect of 30 min isochronal thermal annealing on forward bias *I-V* characteristics. For clarity, only the characteristics for annealing steps ≥250 °C are shown. The inset shows extracted ideality factor for all annealing temperatures.

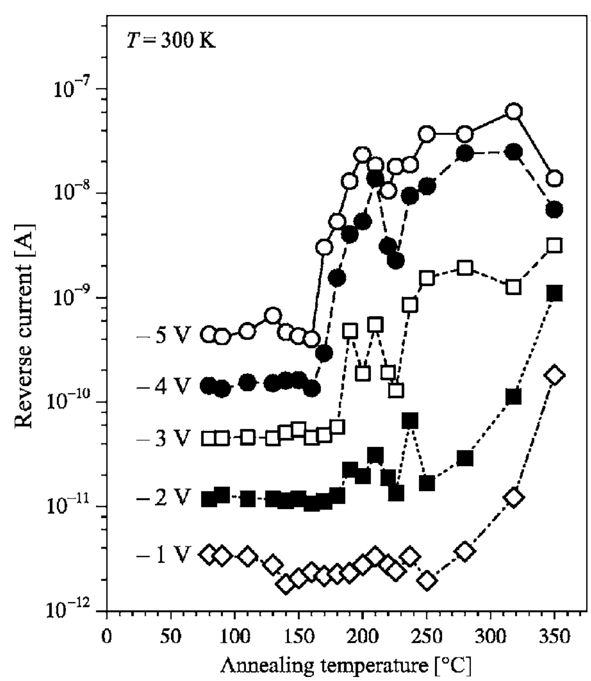

FIG. 4. Degradation of reverse *I-V* characteristics with 30 min isochronal thermal annealing at various reverse bias voltages (bias is indicated next to each curve).

of 47–105 nm, their electrically active cross-sectional area can be much larger and can be affected by biasing conditions.[36,37] Since carrier transport across the metal-semiconductor interface would preferentially occur through localized low-barrier-height regions, the overall *I*-*V* characteristics are characterized by a ϕ_{B0}^{iv} which is lower than the true barrier height of dislocation-free regions and, correspondingly, exhibits an ideality factor that is greater than expected from thermionic-emission theory including image-force barrier-lowering.[46,47] For devices in which interface potential fluctuations are small relative to the depletion depth probed during *C*-*V* measurements (that is, screened out at the edge of the depletion region), the extracted ϕ_B^{cv} represents an average barrier height over the entire diode area, which usually differs significantly from ϕ_{B0}^{iv}.[46,47]

While the differences in extracted values of ϕ_{B0}^{iv} and ϕ_B^{cv}, together with the large values of ideality factor observed for annealing temperatures $>250\ °C$ can be qualitatively explained in terms of localized Schottky-barrier lowering in the vicinity of dislocations,[15] *C*-*V* and *I*-*V* measurements performed on nonirradiated and nonannealed control devices, obtained from the area adjacent to that of the devices employed in this study, indicated that nonidealities in the electrical characteristics of Ni/GaN Schottky diodes can also be attributed to interfacial defects. These control devices exhibited room-temperature ϕ_B^{cv} values of 1.30 ± 0.01 eV which is significantly larger than the Schottky barrier extracted prior to device irradiation ($\phi_B^{cv}=1.05\pm0.05$ eV) but coincides with the barrier height extracted after exposure to a total accumulated gamma-ray dose of 21 Mrad(Si) ($\phi_B^{cv}=1.30\pm0.01$ eV). The values of ϕ_{B0}^{iv} for the control ($\phi_{B0}^{iv}=1.05\pm0.05$ eV) and irradiated devices were consistent. It is noted, however, that significant variations in the extracted room-temperature values of ϕ_B^{cv} where observed in different areas of the same wafer ($0.85-1.30$ eV). This suggests the likely presence of localized regions where the density of interfacial defects is significantly higher than surrounding areas. Given that surface regions in the vicinity of dislocations tend to be more electrically active than regions sufficiently away from them,[36,37] it is likely that high interfacial defect densities in the vicinity of dislocations influence both the behavior of Schottky diodes exposed to energetic irradiation as well as the annihilation of defects during post-irradiation annealing. It should be noted that in this case, dislocations, and their vicinal surface area, are assumed to act as efficient current leakage paths by virtue of their high interfacial density rather than by inducing Schottky-barrier height lowering. While in the latter case the potential fluctuations induced by dislocations would be screened at the edge of the depletion region, the former implies a significantly larger area of influence.

The observed radiation-induced increase in ϕ_B^{cv} after 1 Mrad(Si) can interpreted as arising from either radiation-induced reordering at the metal-GaN interface or to the introduction of a thin layer of acceptor-like interfacial defects which act to compensate donor-like interfacial defects present prior to irradiation. It is noted that both of these scenarios are supported by the observation that deposition of Ni on GaN has been shown to induce V_N-related defects at the metal-GaN interface,[34] in which a thin layer with *n*-type character would be formed. Since V_N defects act as shallow donors,[17,48,49] such an interfacial layer would reduce the width of the space charge layer, causing an increase in depletion capacitance and thus the ϕ_B^{cv} obtained from C^{-2}-*V* characteristics would underestimate ϕ_B^{fb} (as observed in the sample prior to irradiation). In this case, irradiation could induce re-incorporation of N desorbed during metal deposition or from nearby N_I defects produced by irradiation.[34] This argument is supported by the observation of improved GaAs and GaN diode characteristics after relatively low irradiation doses.[11,50] On the other hand, total irradiation doses below 1 Mrad(Si) could induce significant interfacial defect centers via displacement of N and Ga species from their sublattice sites. A net accumulation of acceptor-like defects, such as N_I and V_{Ga} and possibly in N antisites (N_{Ga}), at the interface would induce the appearance of a negatively charged region in the vicinity of the Ni/GaN interface resulting in an increase in ϕ_B^{cv} with irradiation dose. Note that both cases considered take into account the introduction of N-vacancies during Ni deposition.[34] However, of the two mechanisms considered, the case of radiation-induced reordering seems more likely, since it does not require a significant concentration of N_I and/or V_{Ga} at the metal-GaN interface. Furthermore, point acceptor-like defects such as N_I and V_{Ga}, if mobile, have a finite probability of migration into the bulk due to the electric field gradient in the space charge region.

Recent calculations of defect migration barriers indicate that both N_I and V_{Ga} defects are mobile at the annealing temperatures employed in this work.[51] Migration of isolated N_I and V_{Ga} toward the bulk would result in a reduction of carrier concentration. Furthermore, mobile isolated Ga vacancies can become trapped by oxygen atoms substitutional on N sites, O_N, the most likely donor in the nominally undoped GaN layer, resulting in the formation of acceptor-like $V_{Ga}-O_N$ defect complexes, which are known to be immobile in the annealing temperature range herein employed.[7,51] In this case, thermal annealing at sufficiently high temperatures would result in an increase in background acceptor concentration and a net reduction in free carrier concentration, consistent with our observations.

B. Deep-level transient spectroscopy

The DLTS spectra of the radiation-induced defects after exposure to a total ^{60}Co gamma-ray dose of 21 Mrad(Si) are shown in Fig. 5, and their parameters are summarized in Table I. The effect of thermal annealing on the carrier-emission DLTS signal from the three radiation-induced defects is shown in Fig. 6, and the fraction of remaining defects as a function of annealing temperature is presented in Fig. 7. The defect annealing trend exhibited by the three defects was remarkably similar, typically manifesting a sharp defect annihilation transition between 250 and 350 °C, with the annihilation temperature of G_3 being slightly higher than that of G_1 and G_2. A relatively slow stepwise decrease in defect concentration is found to affect the annealing curve of the

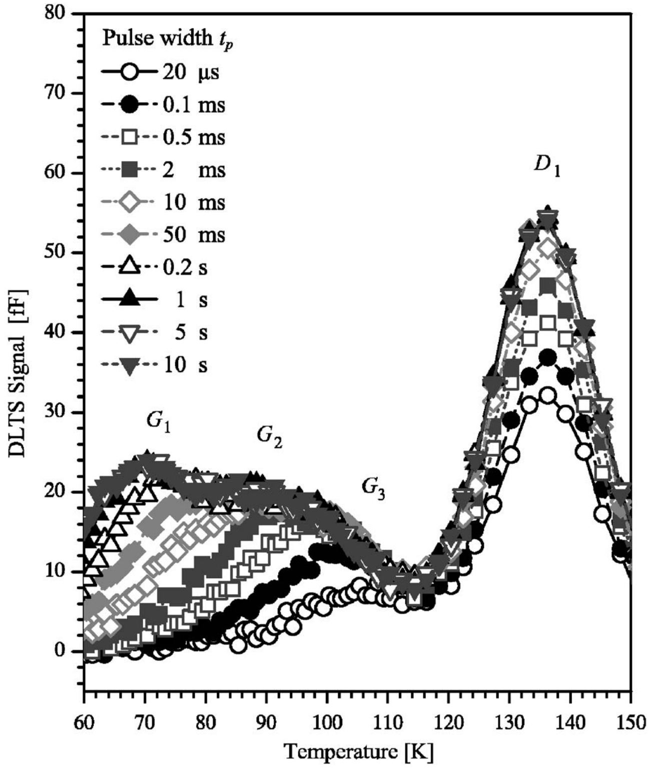

FIG. 5. Evolution of the carrier emission signal of radiation-induced defects with trap-filling pulse duration (t_p) after exposure to a total ^{60}Co gamma ray dose of 21 Mrad(Si) (before annealing). The emission rate window shown is e_n=1.02 s^{-1}.

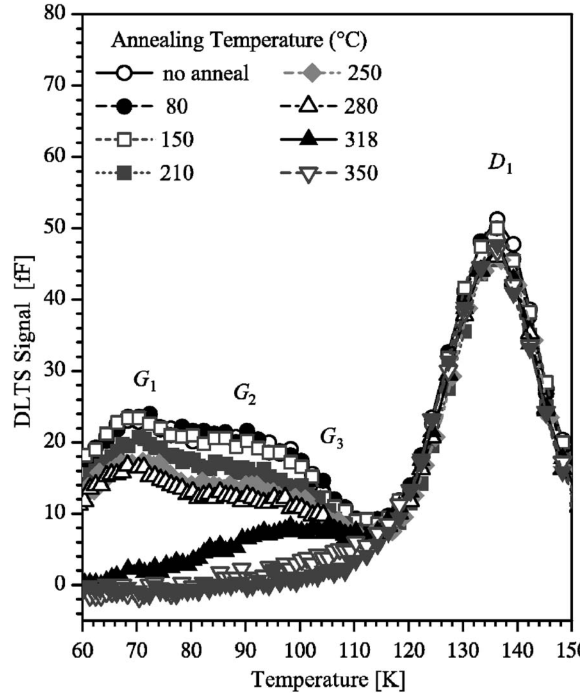

FIG. 6. Evolution of the DLTS signal from radiation-induced defects after 30 min isochronal annealing. For clarity, only selected temperatures are shown. The accumulated gamma ray dose prior to annealing was 21 Mrad(Si), and the emission rate window shown is e_n=1.02 s^{-1}(t_p=10 s).

three defects below 250 °C, with the radiation-induced defects appearing to be stable for annealing temperatures up to 100 °C.

The DLTS measurements were performed using a single value of the trap-filling pulse duration (t_p=10 s), and the DLTS signal of the radiation-induced defects did not manifest any significant shift with annealing temperature, as evident from Fig. 6. Thus, the carrier emission activation energies and capture cross sections of the three radiation-induced defects can be assumed to be essentially unchanged with annealing temperature, which facilitates the extraction of activation energy for defect annihilation process. Assuming that the defect centers produced by irradiation exposure are isolated vacancy and interstitial defects and that mobile defects recombine with their Frenkel-pair counterpart, the isochronal thermal annealing characteristics can be described using a first-order reaction model[52]

$$N_T(T_{i+1}) = N_T(T_i) \times \exp\left\{ - \nu \Delta t \exp\left(- \frac{qE_{TA}}{k_B T_i} \right) \right\}, \quad (5)$$

where $N_T(T)$ is the fraction of remaining defects after annealing at temperature T_i, where i denotes the isochronal step in

TABLE I. Summary of parameters for the defect levels detected in the GaN sample before and after exposure to a total ^{60}Co gamma-ray dose of 21 Mrad(Si) (Ref. 15).

Label	Origin	N_T ($\times 10^{13}$ cm^{-3})	σ_{na} (cm^2)	E_T (meV)
D_1	as-grown	4.3	2.5×10^{-15}	265±7
D_2	as-grown	1.7	6.5×10^{-16}	355±30
D_3	as-grown	61.0	1.4×10^{-15}	581±9
G_1	radiation	3.8	2.6×10^{-18}	88±7
G_2	radiation	3.0	1.2×10^{-18}	104±12
G_3	radiation	2.0	7.6×10^{-18}	144±13

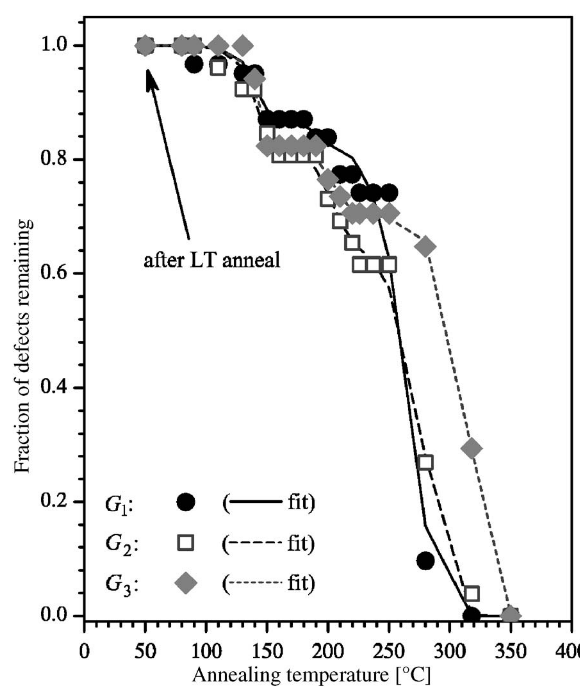

FIG. 7. Fractional change in the concentration of radiation-induced defect as a function of consecutive isochronal thermal annealing steps. Prior to thermal annealing the samples were irradiated to a total ^{60}Co gamma-ray of 21 Mrad(Si). Thermal annealing was performed isochronally (30 min) for temperatures above 80 °C. The arrow indicates the result of a 15 min anneal at 50 °C (see Ref. 15 for more details).

TABLE II. Summary of activation energies, E_{TA}, extracted from the isochronal thermal annealing characteristics of three shallow radiation-induced defects. The ratios indicate the relative influence of different thermally activated defect annihilation processes.

Defect Label	E_{TA} (eV)	Ratio (%)
G_1 (E_a=0.088±0.007 eV)	1.77±0.01	82±4
	1.52±0.05	5±2
	1.35±0.10	12±3
G_2 (E_a=0.104±0.012 eV)	1.80±0.01	66±3
	1.56±0.05	17±5
	1.35±0.04	18±4
G_3 (E_a=0.144±0.013 eV)	1.92±0.01	70±4
	1.57±0.02	13±4
	1.36±0.02	17±4

the order performed (that is, T_i=80,90…350 °C), Δt is the annealing time, ν is a frequency factor ($\nu=10^{13}$ s^{-1} is commonly assumed), and E_{TA} is the activation energy of the process that leads to defect annihilation.[17,52]

To obtain the excellent fit to experimental characteristics shown in Fig. 7, three different defect recombination processes were employed to fit the annealing characteristics of each irradiation-induced level, with the extracted defect annealing parameters presented in Table II. It is noted that the activation energies obtained by independently fitting the defect annealing characteristics below 250 °C are nearly identical, indicating an average activation energy of 1.55±0.04 eV which is consistent with the 1.6 eV barrier energy for migration of N_I calculated by Limpijumnong and Van de Walle,[51] and suggests V_N-N_I pair recombination as the physical mechanism. On the other hand, the dominant annealing process has an activation energy of 1.77–1.92 eV, depending on the specific defect center, which is very close to the calculated energy barrier for the migration of the V_{Ga} defect (1.9 eV).[51] Aside from defect complexing induced by interaction with native O_N donors, V_{Ga} migration may also result in annihilation of V_N by formation of V_{Ga}–V_N divacancies (double acceptor defects), resulting in a corresponding decrease in carrier concentration.[5,7]

It is important to note that the rate at which V_N defects are introduced is expected to be higher than that of V_{Ga} defects, for displacements induced by Compton electrons generated by ^{60}Co gamma-rays.[17] Given that calculated energy barriers for the migration V_N and N_I defects are relatively high (4.3 and 1.6 eV, respectively[51]) such defects would be expected to be relatively immobile during irradiation or for annealing temperatures below 100 °C (neglecting any possible radiation-induced enhancement in defect mobility). In contrast, the relatively low energy for the migration of the Ga_I defect (0.9 eV) could lead to recombination of radiation-induced $V_{Ga}-N_{Ga}$ during radiation exposure, or to the formation of complex defects. On the other hand, and taking into account that Ga_I is the only radiation-induced lattice point defect known to be mobile at room temperature,[2,5,6,51] it is likely that Ga_I plays a significant role in the post-irradiation recovery of the reverse *I-V* characteristics observed after prolonged storage at room temperature, and for annealing temperatures up to 160 °C.

While the above discussion is centered on the view that the observed radiation-induced defect centers are due to displacement of N or Ga species from their respective sublattices, gamma-irradiation is also capable of inducing ionization effects that are not readily observable when employing monoenergetic electron-beam irradiation.[53] Ionization effects are likely to exert a significant influence on the mobility of defects and impurities during irradiation, since the increase in electron and hole populations during irradiation exposure can alter their charge state. In this regard, hydrogen-related defects are of particular interest because hydrogen is abundantly present in many of the techniques used for growth of GaN.[54,55] Furthermore, H is an amphoteric defect which has a relatively low migration barrier (0.9–1.4 eV) when in the H^+ charge state, its formation is favorable under *p*-type growth conditions.[56,57] Under the thermodynamic equilibrium conditions of *n*-type growth, H^+ has a high formation energy and H^- is favored. However, H^- has a high barrier for migration (2–2.2 eV).[56,57] Thus, the mobility of the hydrogen species depends on its charge state and on the Fermi level position.[56,57] Since as-grown *n*-GaN is likely to have a high concentration of relatively immobile H^-, the change in Fermi level induced during irradiation can induce a change from H^- to H^+ by emission of two electrons. Thus, the presence of highly mobile H^+ species during irradiation could lead to passivation of acceptor-like defect centers such as isolated V_{Ga}^{-3} or N_I^- defects or $(V_N-O_N)^{-2}$ complexes (regardless of their origin as intrinsic or radiation-induced defects). While the experimental results presented in this paper cannot be directly correlated with the above mechanisms, hydrogen-related defect activation and/or migration during irradiation is likely to be an important mechanism given that hydrogen-related vibrational-modes have been observed to be activated in *n*-GaN films exposed to ^{60}Co gamma-radiation.[58,59]

Although it is difficult to attribute the effects observed in the *I-V* and *C-V* characteristics to the migration of any particular defect, the DLTS results clearly indicate that thermal annealing leads to annihilation of the shallow radiation-induced V_N-related defects. Given that defect migration energy barriers are likely to be affected by the local environment of the defect, we can associate the dominant annihilation mechanism to a mean activation energy of 1.80±0.13 eV, obtained by taking into account the various defect concentrations. It is noted that the observed annealing behavior of the irradiation-induced defects is consistent with the results of Look *et al.*, who extracted activation energies in the 1.67–2.12 eV range from the thermal-annealing-induced recovery of the electron mobility at 80 K in *n*-GaN films exposed to 1 MeV electron-irradiation. However, in view of the recent theoretical calculations included in the above discussion, it is not clear whether the mean activation energy of 1.80±0.13 eV can be attributed to the migration energy barrier for the N_I^- defect, which Limpijumnong and Van de Walle have calculated to be 1.6 eV.[51]

IV. SUMMARY AND CONCLUSIONS

Isochronal thermal annealing at temperatures from 80 to 350 °C, performed following a low-temperature anneal (6 days at room temperature plus 15 min. at 50 °C), was found to induce complete annihilation of radiation-induced defects, while inducing an accumulated 7% decrease in free carrier concentration after the 350 °C anneal. Annealing at temperatures up to 150 °C was found to improve the *I-V* in characteristics, while annealing at temperatures above 150 °C was found to induce degradation in reverse leakage current. However, annealing at temperatures in excess of 250 °C was found to induce significant degradation in both forward and reverse *I-V* device characteristics. While DLTS measurements indicated that the defect parameters and thermal annealing characteristics of the radiation-induced defects are consistent with defects previously attributed to nitrogen-vacancy related centers,[17] the activation energy of the defect annihilation process, 1.80±0.13 eV, differs from the theoretical energy barriers for the migration of nitrogen interstitial and vacancy defects (1.6 and 4.3 eV, respectively[51]).

ACKNOWLEDGMENT

The authors wish to acknowledge the financial support of this project by the Australian Research Council (ARC).

[1] U. K. Mishra, Y.-F. Wu, B. P. Keller, S. Keller, and S. P. DenBaars, IEEE Trans. Microwave Theory Tech. **46**, 756 (1998).
[2] K. H. Chow, G. D. Watkins, A. Usui, and M. Mizuta, Phys. Rev. Lett. **85**, 2761 (2000).
[3] M. Linde, S. J. Uftring, and G. D. Watkins, Phys. Rev. B **55**, R10177 (1997).
[4] C. Bozdog, H. Przybylinska, G. D. Watkins, V. Härle, F. Scholz, M. Mayer, M. Kamp, R. J. Molnar, A. E. Wickenden, D. D. Koleske *et al.*, Phys. Rev. B **59**, 12479 (1999).
[5] K. H. Chow, L. S. Vlasenko, P. Johannesen, C. Bozdog, G. D. Watkins, A. Usui, H. Sunakawa, C. Sasaoka, and M. Mizuta, Phys. Rev. B **69**, 045207 (2004).
[6] P. Johannesen, A. Zakrzewski, L. S. Vlasenko, G. D. Watkins, A. Usui, H. Sunakawa, and M. Mizuta, Phys. Rev. B **69**, 045208 (2004).
[7] K. Saarinen, T. Suski, I. Grzegoryba, and D. C. Look, Physica B **308–310**, 77 (2001).
[8] S. Hautakangas, J. Oila, M. Alatalo, K. Saarinen, L. Liszkay, D. Seghier, and H. Gislason, Phys. Rev. Lett. **90**, 137402 (2003).
[9] I. A. Buyanova, M. Wagner, W. M. Chen, B. Monemar, J. L. Lindström, H. Amano, and I. Akasaki, Appl. Phys. Lett. **73**, 2968 (1998).
[10] A. Ionascut-Nedelcescu, C. Carlone, A. Houdayer, H. J. von Bardeleben, J.-L. Cantin, and S. Raymond, IEEE Trans. Nucl. Sci. **49**, 2733 (2002).
[11] C.-W. Wang, J. Vac. Sci. Technol. B **20**, 1821 (2002).
[12] S. J. Cai, Y. S. Tang, R. Li, Y. Y. Wei, L. Wong, Y. L. Chen, K. L. Wang, M. Chen, Y. F. Zhao, R. D. Schrimpf *et al.*, IEEE Trans. Electron Devices **47**, 304 (2000).
[13] S. M. Khanna, J. Webb, A. J. Houdayer, and C. Carlone, IEEE Trans. Nucl. Sci. **47**, 2322 (2000).
[14] F. Gaudreau, C. Carlone, A. Houdayer, and S. M. Khanna, IEEE Trans. Nucl. Sci. **48**, 1778 (2001).
[15] G. A. Umana-Membreno, J. M. Dell, B. D. Nener, G. Parish, L. Faraone, and U. K. Mishra, IEEE Trans. Electron Devices **50**, 2326 (2003).
[16] S. A. Vitusevich, N. Klein, A. E. Belyaev, S. V. Danylyuk, M. V. Petrychuk, R. V. Konakova, A. M. Kurakin, A. E. Rengevich, A. Y. Avksentyev, B. A. Danilchenko *et al.*, Phys. Status Solidi A **195**, 101 (2003).
[17] D. C. Look, D. C. Reynolds, J. W. Hemsky, J. L. Sizelove, R. L. Jones, and R. J. Molnar, Phys. Rev. Lett. **79**, 2273 (1997).
[18] V. V. Emtsev, V. Y. Davydov, V. V. Kozlovskii, V. V. Lundin, D. S. Poloskin, A. N. Smirnov, N. M. Schmidt, A. S. Usikov, J. Aderhold, H. Klausing *et al.*, Semicond. Sci. Technol. **15**, 73 (2000).
[19] D. C. Look, G. C. Farlow, P. J. Drevinsky, D. F. Bliss, and J. L. Sizelove, Appl. Phys. Lett. **83**, 3525 (2003).
[20] Z. Q. Fang, L. Polenta, J. W. Hemsky, and D. C. Look, SIMC-IX Proceedings, 2000, pp. 35–42.
[21] L. Polenta, Z.-Q. Fang, and D. C. Look, Appl. Phys. Lett. **76**, 2086 (2000).
[22] S. A. Goodman, F. D. Auret, M. J. Legodi, G. Myburg, B. Beaumont, and P. Gibart, SIMC-IX Proceedings, 2000, pp. 43–46.
[23] P. V. Dressendorfer, in *Ionization Effects in MOS Devices and Circuits*, edited by T. P. Ma and P. V. Dressendorfer (Wiley, New York, 1989), Chap. 6, pp. 333–400.
[24] B. T. Kelly, *Irradiation Damage to Solids* (Pergamon, New York, 1966), Chap. 2, pp. 72–117.
[25] Z.-Q. Fang, J. W. Hemsky, D. C. Look, and M. P. Mack, Appl. Phys. Lett. **72**, 448 (1998).
[26] S. Goodman, F. Auret, F. Koschnick, J.-M. Spaeth, B. Beaumont, and P. Gibart, Mater. Sci. Eng., B **71**, B100 (2000b).
[27] B. P. Keller, S. Keller, D. Kapolnek, W.-N. JIang, Y.-F. Wu, H. Masui, X. Wu, B. Heying, J. S. Speck, U. K. Mishra, *et al.*, J. Electron. Mater. **24**, 1707 (1995).
[28] E. H. Rhoderick and R. H. Williams, *Metal-Semiconductor Contacts* (Clarendon, Oxford, 1988), Chap. 3, pp. 89–140.
[29] L. S. Yu, Q. Z. Liu, Q. J. Qiao, S. S. Lau, and J. Redwing, J. Appl. Phys. **84**, 2099 (1998).
[30] J. C. Carrano, T. Li, P. A. Grudowski, C. J. Eiting, R. D. Dupuis, and J. C. Campbell, J. Appl. Phys. **83**, 6148 (1998).
[31] T. Sawada, Y. Ito, K. Imai, K. Suzuki, H. Tomozawa, and S. Sakai, Appl. Surf. Sci. **159-160**, 449 (2000).
[32] H. Hasegawa and S. Oyama, J. Vac. Sci. Technol. B **20**, 1647 (2002).
[33] V. M. Bermudez, R. Kaplan, M. A. Khan, and J. N. Kuznia, Phys. Rev. B **48**, 2436 (1993).
[34] M. H. Kim, S. N. Lee, C. Huh, S. Y. Park, J. Y. Han, J. M. Seo, and S. J. Park, Phys. Rev. B **61**, 10966 (2000).
[35] A. Barinov, L. Gregoriatti, B. Kaulich, M. Kiskinova, and A. Rizzi, Appl. Phys. Lett. **79**, 2752 (2001).
[36] E. G. Brazel, M. A. Chin, and V. Narayamurti, Appl. Phys. Lett. **74**, 2367 (1999).
[37] J. W. P. Hsu, M. J. Manfra, D. V. Lang, S. Richter, S. N. G. Chu, A. M. Sergent, R. N. Kleinman, L. N. Pfeiffer, and R. J. Molnar, Appl. Phys. Lett. **78**, 1685 (2001).
[38] J. W. P. Hsu, H. M. Ng, A. M. Sergent, and S. N. G. Chu, Appl. Phys. Lett. **81**, 3579 (2002).
[39] J. D. Guo, F. M. Pan, M. S. Feng, R. J. Guo, P. F. Chou, and C. Y. Chang, J. Appl. Phys. **80**, 1623 (1996).
[40] Q. Z. Liu and S. S. Lau, J. Appl. Phys. **84**, 881 (1998).
[41] K. Shiojima, J. M. Woodall, C. J. Eiting, P. A. Grudowski, and R. D. Dupuis, J. Vac. Sci. Technol. B **17**, 2030 (1999).
[42] J. Spradlin S. Doğan, J. Xie, R. Molnar, A. A. Baski, and H. Morkoc, Appl. Phys. Lett. **84**, 4150 (2004).
[43] B. S. Simpkins, E. T. Yu, P. Waltereit, and J. S. Speck, J. Appl. Phys. **94**, 1448 (2003).
[44] R. Jones, J. Elsner, M. Haugk, R. Gutierrez, T. Frauenheim, M. Heggie, S. Öberg, and P. Briddon, Phys. Status Solidi A **171**, 167 (1999).
[45] I. Arslan and N. D. Browning, Phys. Rev. Lett. **91**, 165501 (2003).
[46] J. H. Werner and H. H. Güntler, J. Appl. Phys. **69**, 1522 (1991).
[47] R. T. Tung, Mater. Sci. Eng., R. **R35**, 1 (2001).
[48] P. Bogusławski, E. L. Briggs, and J. Bernholc, Phys. Rev. B **51**, 17255 (1995).
[49] J. Neugebauer and C. G. Van de Walle, Phys. Rev. B **50**, 8067 (1994).
[50] O. Y. Borkovskaya, N. L. Dmitruk, R. V. Konakova, V. G. Litovchenko, and O. I. Maeva, Sov. Phys. Semicond. **20**, 1028 (1986).
[51] S. Limpijumnong and C. G. V. de Walle, Phys. Rev. B **69**, 035207 (2004).
[52] B. T. Kelly, *Irradiation Damage to Solids* (Pergamon, New York, 1966), Chap. 4, pp. 179–209.
[53] G. C. Messenger and M. S. Ash, *The Effects of Radiation on Electronic Systems* (Van Nostrand Reinhold, New York, 1992), Chap. 6, pp. 269–359.
[54] O. Ambacher, H. Angerer, R. Dimitrov, W. Rieger, M. Stutzmann, G. Dollinger, and A. Bergmaier, Phys. Status Solidi A **159**, 105 (1997)
[55] M. G. Weinstein, F. Jaing, M. Stavola, B. Bech Neilsen, A. Usui, and M. Mizuta, Physica B **308–310**, 122 (2001).
[56] S. Limpijumnong and C. G. Van de Walle, Phys. Rev. B **68**, 235203 (2003).
[57] C. G. Van de Walle and J. Neugebauer, J. Appl. Phys. **95**, 3851 (2004).
[58] J. Q. Duan, B. R. Zhang, Y. X. Zhang, L. P. Wang, G. G. Qin, G. Y. Zhang, Y. Z. Tong, S. X. Jin, Z. J. Yang, X. Zhang *et al.*, J. Appl. Phys. **82**, 5745 (1997).
[59] W. H. Sun, L. S. Wang, S. J. Chua, K. M. Chen, and G. C. Qin, Mater. Sci. Semicond. Process. **4**, 559 (2001).